
**Liquid Crystals**
Publication details, including instructions for authors and subscription information:
http://www.informaworld.com/smpp/title~content=t713926090

# Perturbative analysis of the magnetic field effect on the stability of the shear flow of a nematic polymer

J. L. Figueirinhas[ab]; J. P. Casquilho[cd]
[a] Centro de Física da Matéria Condensada - Universidade de Lisboa, 1649-003 Lisboa, Portugal [b] Dep. de Física, Instituto Superior Técnico, 1049-001 Lisboa, Portugal [c] Dep. de Física, [d] CENIMAT, Faculdade de Ciências e Tecnologia da Universidade Nova de Lisboa, Monte da Caparica 2829-516 Caparica Portugal,

**To cite this Article** Figueirinhas, J. L. and Casquilho, J. P.(2008) 'Perturbative analysis of the magnetic field effect on the stability of the shear flow of a nematic polymer', Liquid Crystals, 35: 4, 501 — 505
**To link to this Article: DOI:** 10.1080/02678290801956347
**URL:** http://dx.doi.org/10.1080/02678290801956347

*Liquid Crystals*,
Vol. 35, No. 4, April 2008, 501–505



# Perturbative analysis of the magnetic field effect on the stability of the shear flow of a nematic polymer

J. L. Figueirinhas[ab]* and J. P. Casquilho[cd]

[a]*Centro de Física da Matéria Condensada - Universidade de Lisboa, Av. Prof. Gama Pinto 2, 1649-003 Lisboa, Portugal;* [b]*Dep. de Física, Instituto Superior Técnico, Av. Rovisco Pais, 1049-001 Lisboa, Portugal;* [c]*Dep. de Física;* [d]*CENIMAT, Faculdade de Ciências e Tecnologia da Universidade Nova de Lisboa, Monte da Caparica 2829-516 Caparica Portugal*

*(Received 7 December 2007; final form 30 January 2008)*

The effect was investigated of an applied magnetic field on the stability of the shear flow of a nematic polymer liquid crystal of the tumbling type with respect to the formation of transient bands. For a given Ericksen number of the flow, the critical field that suppresses the thermally generated and shear amplified perturbations is calculated. The boundary in the control parameter space between the homogeneous and the band formation regime is calculated using a numerical simulation of the flow based on a time-dependent perturbative analysis. It is also found that the critical wavevector of the bands increases with the field and decreases with the Ericksen number of the flow and with the shear strain when a magnetic field is applied.

**Keywords:** perturbative analysis; magnetic field effect; shear flow; nematic polymer



## 1. Introduction

In this paper, the effect of an applied magnetic field on the stability of the shear flow of a nematic polymer of the tumbling type with respect to the formation of the transient bands that appear after the start-up of shearing is studied using the Ericksen–Leslie (EL) nematodynamics theory (*1*). Banded textures have been observed as a transient response to the start-up of the shearing of nematic liquid crystalline polymers when the initial orientation of the director is homeotropic (*2*). The mechanism of the formation of the transient bands as a response to flow relies on the fact that most polymer nematics are of the tumbling type (*3, 4*). For such materials, the flow-induced orientation distortion stores a large amount of elastic energy that needs to be relaxed, giving way to an in-plane instability (tumbling of the nematic director) or to an out-of-plane instability where the director tends to align along the vorticity axis of the flow and hence avoid the increasing torques associated with larger shear stresses. This out-of-plane component of the director may be homogeneous in space or periodic, in this case giving rise to a banded pattern. The analysis of these shear-induced instabilities, being a significant subject in the science of polymer liquid crystals (PLCs), has attracted considerable attention (*2–10*) and was modelled with the help of Rheo-Optics by Rey and co-workers (*11, 12*) and of Rheo-RMN by Martins and co-workers (*13, 14*). The suppression of these instabilities is a relevant subject for the processing of these materials and we investigate in this work the effect of an external magnetic field on the onset and growth conditions of the instabilities.

In a previous paper (*15*), a linear stability analysis of the stationary solution of the equations for the shear flow of tumbling nematic polymers in the suppressed tumbling regime, with homeotropic boundary conditions and a magnetic field applied orthogonally to the sample plane, was reported. This analysis allowed a qualitative description to be obtained of the role of the magnetic field and of the boundaries in the stability of the flow with respect to the formation of the transient bands orthogonal to the shearing direction. In this work a time-dependent perturbative analysis of the flow equations is carried out for the same geometry (defined in Figure 1) with the goal of determining the boundary in the control parameter space between the homogeneous and the band-formation regimes and to obtain an insight into the dependence on time and shear strain of the flow behaviour under an applied magnetic field. This analysis is appropriate to determine the transition line in the phase diagram of the control parameter space.

## 2. Mathematical model

In order to study the stability of the basic flow with respect to the formation of spatially periodic patterns, we consider the presence of thermally excited periodic perturbations in the director and velocity

*Corresponding author. Email: figuei@cii.fc.ul.pt

ISSN 0267-8292 print/ISSN 1366-5855 online

DOI: 10.1080/02678290801956347
http://www.informaworld.com

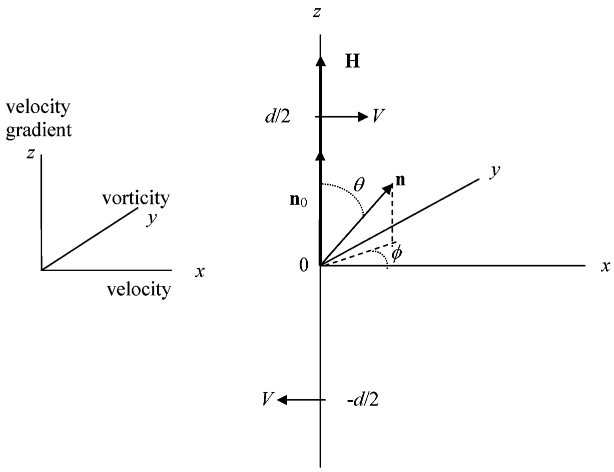


Figure 1. Definition of the sample geometry: the plates are at $z=\pm d/2$. $\mathbf{n}_0$ is the initial uniform director field and **n** its direction at a given instant during the flow. **H** is applied in the shearing plane and orthogonally to the sample plates. The shearing plane is defined as the plane containing the flow and the flow gradient. $V$ is the velocity of the plates.

fields and compute the time dependence of those modes that are amplified, corresponding to the selected wavevector at each instant. More specifically, we integrate the linearised EL equations for the perturbations of the director and the velocity fields from zero up to a time $t$, for a specific value of the wavevector **q**, using the nonlinear director and velocity fields obtained from the basic shear flow. The initial conditions for the perturbations are obtained generating thermal noise. For each given time value $t$, the perturbation amplitude is maximised over **q**. The maximising **q** is retained along with the maximised amplitudes of the perturbations of the director and the velocity fields. The details of this method can be found elsewhere (*16*). Our numerical results are obtained in the suppressed tumbling regime due to the boundary and/or the magnetic field effects.

In our model the director and velocity fields are parameterised by an ansatz that considers the flow as a composition of the basic flow with the director ***n*** and fluid velocity ***v*** in the shearing plane and a periodic perturbation in both the velocity and the director with components also in the vorticity direction. The director, fluid velocity, pressure and magnetic fields are defined in Figure 1 and are given by:

$$H_x=0\ ,\ H_y=0,\ H_z=H; \qquad (1a)$$

$$v_x(x,y,z,t)=v_x^0(z,t)+v_x^1(x,y,z,t); \qquad (1b)$$

$$v_y(x,y,z,t)=v_y^1(x,y,z,t),\ v_z=0; \qquad (1c)$$

$$p(x,y,z,t)=p^0(z,t)+p^1(x,y,z,t); \qquad (1d)$$

$$\mathrm{n_x}=\sin\left(\theta^0(\mathrm{z,t})\right),\ \mathrm{n_y}=\phi^1(\mathrm{x,y,z,t}),\ \mathrm{n_z}=\cos\left(\theta^0(\mathrm{z,t})\right). \qquad (1e)$$

The *ansatze* used for $v^0{}_x$, $\theta^0$ and $p^0$ describing the velocity, the director field and the pressure in the basic flow are:

$$v_x^0(\mathrm{z,t})=\dot\gamma\ z+v_\beta(t)\sin(2q_z z); \qquad (2)$$

$$\theta^0(z,t)=\theta_\alpha(t)\cos(q_z z)+\theta_\beta(t)\cos(3q_z z); \qquad (3)$$

$$p^0(z,t)=p^a(z,t), \qquad (4)$$

where

$$\dot\gamma=\frac{v_x(z=d/2)}{d/2} \qquad (5)$$

is the shear rate and the boundary conditions are set through the relation

$$q_z=\pi/d,\ z\in\{-d/2,\ d/2\}. \qquad (6)$$

To attain a better description of the basic flow, the *ansatze* given in Equations (2) and (3) include beyond the lowest order terms giving the $z$ dependence of $v^0{}_z$ and $\theta^0$ compatible with the boundary conditions and considered previously (*15*), the next higher order terms also compatible with the symmetry of the problem.

The *ansatze* used for the perturbations are:

$$\phi^1(x,y,z,t)=\phi(t)\exp\left(I\left(q_x x+q_y y\right)\right)\cos(q_z z); \qquad (7)$$

$$v_x^1(x,y,z,t)=v_\xi(t)\exp\left(I\left(q_x x+q_y y\right)\right)Iq_y\cos(q_z z); \qquad (8)$$

$$v_y^1(x,y,z,t)=-v_\xi(t)\exp\left(I\left(q_x x+q_y y\right)\right)Iq_x\cos(q_z z), \qquad (9)$$

where $q_x$ and $q_y$ are the $x$ and $y$ components of the wavevector of the distortion and $I=\sqrt{-1}$. These *ansatze* for the perturbations represent periodic modulations of the director and velocity fields with wavevector in $x$–$y$ plane and obey strong boundary conditions at $z=\pm d/2$. With Equations (1), (2), (8) and (9) the incompressibility condition is obeyed.

For determining the fluid velocity $\boldsymbol{v}$, the director $\mathbf{n}$ and the pressure $p$ in the basic flow, Equations (1) with the *ansatze* given by Equations (2)–(4) substituted in (without the perturbations) were plugged in the six E–L equations, i.e. the three velocity equations

$$\rho \frac{d}{dt} v_i = \partial_j \sigma_{ji}, \tag{10}$$

where $\sigma_{ji}$ is the stress tensor (*1*); the two independent director equations which, upon neglecting the inertial term, reduce to a balance of torques equations:

$$\partial_j \pi_{ji} - \frac{\partial F_d}{\partial n_i} + \chi_a (\mathbf{n}.\mathbf{H}) H_i = \Gamma_i^{visc}, \tag{11}$$

where in the elastic torque $\pi_{ji}$ is the Ericksen tensor and $F_d$ the Frank distortion free energy (*1*), in the magnetic torque $\chi_a$ is the anisotropy of the magnetic susceptibility, and $\Gamma^{\text{visc}}$ is the viscous torque (*1*). The sixth equation is the incompressibility condition

$$\text{div } v = 0. \tag{12}$$

One then obtains three independent equations (two coming from the velocity equations and the third coming from the director equations) on the time functions $v_\beta(t)$, $\theta_\alpha(t)$, $\theta_\beta(t)$ and the pressure $p^a(z,t)$. The pressure shows up in only one of the velocity equations, the other two equations are evaluated at $z=d/4$ where the periodic term in the velocity is a maximum. The director equation is also evaluated at $z=0$ and this produces the set of three ordinary differential equations that are solved numerically for $v_\beta(t)$, $\theta_\alpha(t)$ and $\theta_\beta(t)$ with a fifth-order Cash-Karp Runge–Kutta algorithm (*17*) starting from a zero velocity and homeotropic director alignment configuration. $v_\beta(t)$, $\theta_\alpha(t)$ and $\theta_\beta(t)$ thus found are then substituted in the linearised EL equations on the perturbation amplitudes $v_\xi(t)$ and $\phi(t)$, where the perturbation on the pressure is cancelled out by the application of the rotational operator on both sides of the velocity equations. The two linearly independent ordinary differential equations of motion for the variables $v_\xi(t)$ and $\phi(t)$ are chosen from the resulting set of linear equations as those that are not identically null at the onset of flow (one coming from the director equation and other from the velocity equation). The equations are solved numerically for a non-dimensional time, defined by $\dot{\gamma}.t$, that is the shear strain is $\gamma_c$. Two non-dimensional numbers show up, which are the control parameters in this problem: the Ericksen number of the flow

$$\text{Er} = \frac{\gamma_1 \dot{\gamma} d^2}{K_3} \tag{13}$$

and the reduced field

$$h = \frac{H}{H_c},\ H_c = \sqrt{\frac{K_3 \pi^2}{\chi_a d^2}}, \tag{14}$$

where the anisotropy of the magnetic susceptibility, $\chi_a$, cancels out of the non-dimensional form of the equations.

## 3. Results

The numerical simulations were evaluated with the viscoelastic parameters of the lyotropic solution of ploy-$\beta$-benzylglutomate (PBG) shown in Table 1, which is of the tumbling type. The results of this analysis on the effect of the applied magnetic field on the stability of the shear flow are expected on physical grounds. The increase of the critical Ericksen number (for the amplification of the periodic modes) with the field, as shown in Figure 2, reflects the stabilising effect of the field over the flow, because higher magnetic fields require higher shear rates for the onset of the instabilities. The (reduced) time evolution of the director perturbation in the vicinity of the boundary between regions I and II shows a blip before increasing/decreasing with the time, which allows results to be obtained referred to this local maximum. Further under/above the transition line this blip no longer exists and the perturbation grows/decays exponentially with time.

The shear strain at the maximum of the distortion increases with Er for all the studied values of the field, as shown in Figure 3. The shear strain dependence of the director perturbation maximum amplitude is shown in Figure 5.

The non-vanishing component of the critical reduced wavevector, $q_{xr}=q_x/q_z$, that results in bands (orthogonal to the shear direction) as observed experimentally (*2*), increases with the field and decreases with the Ericksen number and with the

Table 1. Parameters of PBG used in the numerical simulations (*19*).

| Viscosities/g cm$^{-1}$ s$^{-1}$ | Elastic constants/dyn |
|---|---|
| $\alpha_1=-36.7$ | $K_1/K_2=15.5$ |
| $\alpha_2=-69.2$ | $K_3/K_2=9.78$ |
| $\alpha_3=0.20$ | $K_2=0.78\times10^{-7}$ |
| $\alpha_4=3.48$ | |
| $\alpha_5=66.1$ | |

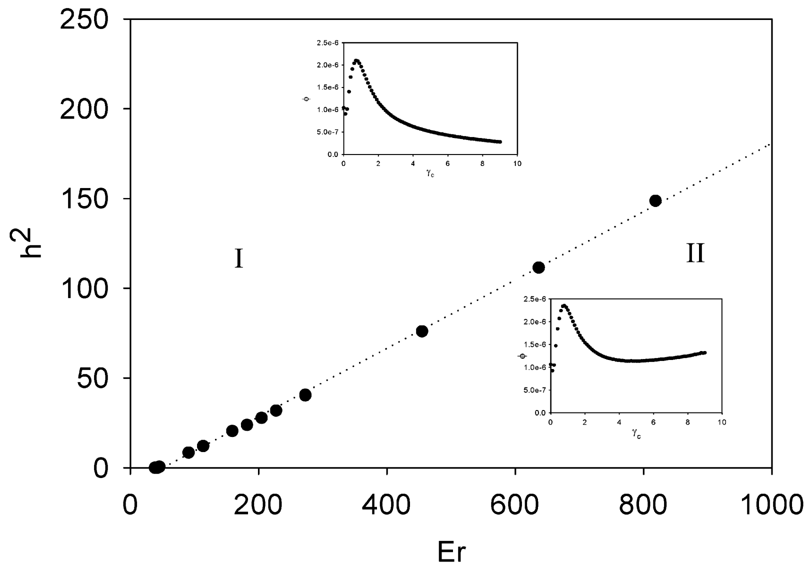


Figure 2. Band formation diagram in the (Er,$h$) control parameter space at the onset of shear. In region I the director thermal fluctuations are attenuated during the shear. In region II the director thermal fluctuations are amplified. Insets show examples of the blip in the perturbation as a function of reduced time in the vicinity of the transition line.



shear strain when a magnetic field is applied, as shown in Figures 4 and 6. The first behaviour should be understood in terms of a balance between the magnetic energy and the elastic energy associated with the periodic distortion such that the increasing of the magnetic field allows for a smaller band wavelength, which is a well known feature of the magnetic field induced linear mode (*18, 19*). The similar behaviour with the Ericksen number and with the shear strain is due to both Er and $\gamma_c$ being proportional to the shear rate: our results give then a selected wave vector that is (approximately) independent of the shear rate for zero applied magnetic field, which reflects a balance between the viscous flow energy and the elastic energy such that the wavelength of the shear induced periodic distortions in polymer nematics should reach a value that is independent of $\dot{\gamma}$ (*2, 3*). When a magnetic field is applied, the behaviour of the wavevector with Er and $\gamma_c$ should reflect a non trivial interplay between these three energies. As found previously (*15*), the critical wavelength of the transient bands during shear is found to be invariant for constant (Er,$h$).

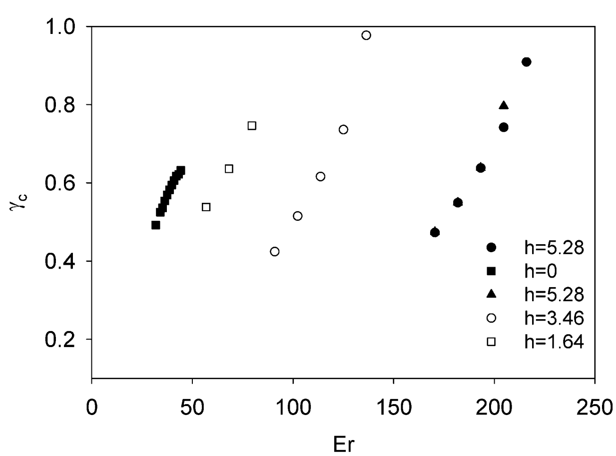


Figure 3. Ericksen number dependence of the shear strain, $\gamma_c = \dot{\gamma}.t$, corresponding to the maximum amplitude of the transient bands appearing at the onset of shear in the vicinity of the boundary between regions I and II. The data sets were obtained with $q_z = 628.318\,\mathrm{cm}^{-1}$, except the full circles (for $h = 5.28$), which were obtained with $q_z = 314.159\,\mathrm{cm}^{-1}$.

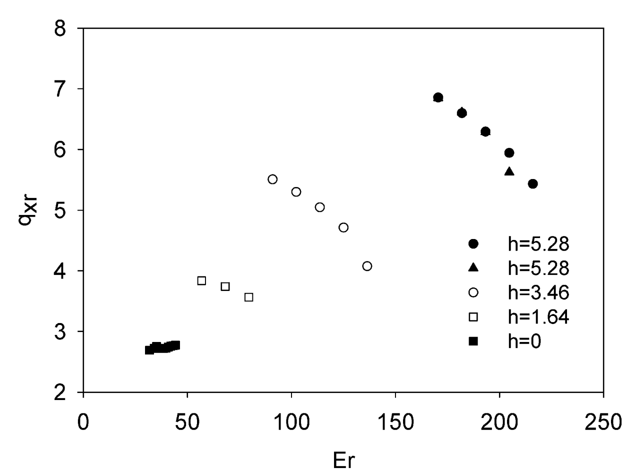


Figure 4. Ericksen number dependence of the reduced wavevector at the reduced time corresponding to the maximum amplitude of the transient bands appearing at the onset of shear, in the vicinity of the boundary between regions I and II. The data sets were obtained with $q_z = 628.318\,\mathrm{cm}^{-1}$, except the full circles (for $h = 5.28$), which were obtained with $q_z = 314.159\,\mathrm{cm}^{-1}$.

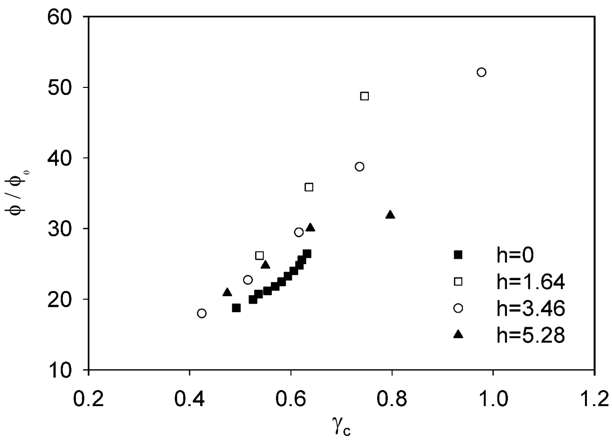


Figure 5. Shear strain dependence of the ratio of the maximum amplitude of the perturbation *vs.* the initial amplitude generated as thermal noise.

## 4. Conclusion

The numerical simulations for the shear flow of a PBG nematic slab show that the thermally excited, time-dependent periodic modes are amplified during the director reorientation process only if the magnetic field is smaller than a critical value for a given value of the Ericksen number of the flow. This is shown in the control parameter (Er,$h$) phase diagram depicted in Figure 2. The use of an external magnetic field may then be an effective way of suppressing the onset of these instabilities in the flow. The perturbative analysis used in this work allowed for the study of the formation and early time evolution of the shear induced transient bands in the vicinity of the boundary in the phase diagram. In this vicinity the perturbation amplitude is small enough to validate the linear approximation thus allowing the transition line to be obtained between the homogeneous and the band formation regimes. To explore this diagram further under the transition line an expansion in the perturbations up to a higher order seems necessary, such that nonlinear terms can allow for saturating and eventually decaying of the otherwise exponential growth of the linear perturbations.

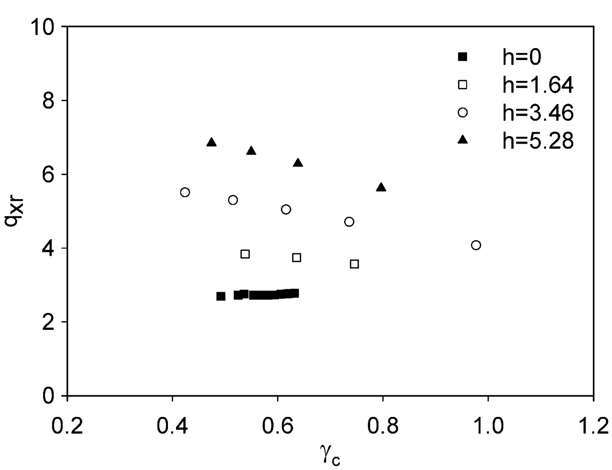


Figure 6. Shear strain dependence of the critical reduced wavevector of the distortion.



## Acknowledgements

This work was supported in part by the Fundação para a Ciência e a Tecnologia of Portugal under Research Contract POCI/CTM/61293/2004.

## References

(1) de Gennes P.G.; Prost J. *The Physics of Liquid Crystals*, 2nd ed,; Clarendon Press: Oxford, 1993.
(2) Larson R.G.; Mead D.W. *Liq. Cryst.* **1992**, *12*, 751–768; Larson, R.G. In *Spatio-Temporal Patterns*, 219–228; Cladis, P.E., Palffy-Muhoray, P., Eds.; SFI Studies in the Sciences of Complexity; Addison-Wesley: 1995.
(3) Burghardt W.R.; Fuller G.G. *J. Rheol* **1990**, *34*, 959–992.
(4) Marrucci G. In *Rheology and Processing of Liquid Crystal Polymers*; Acierno, D., Collyer, A.A., Eds.; Chapman & Hall: 1996.
(5) Zuniga I.; Leslie F.M. *Liq. Cryst.* **1989**, *5*, 725–734.
(6) Srinivasaro M.; Berry G.C. *J. Rheol.* **1991**, *35*, 379–397.
(7) Han W.H.; Rey A.D. *J. non-Newtonian Fluid Mech.* **1993**, *48*, 181–210.
(8) Han W.H.; Rey A.D. *J. non-Newtonian Fluid Mech.* **1993**, *50*, 1–28.
(9) Yan N.X.; Labes M.M.; Baek S.G.; Magda J.J. *Macromolecules* **1994**, *27*, 2784–2788.
(10) Vermant J.; Moldenaers P.; Picken S.J.; Mewis J. *J. non-Newtonian Fluid Mech.* **1994**, *53*, 1–23.
(11) Han W.H.; Rey A.D. *Macromolecules* **1995**, *28*, 8401–8405.
(12) Hwang D.K.; Han W.H.; Rey A.D. *J. non-Newtonian Fluid Mech.* **2007**, *143*, 10–21.
(13) Polimeno A.; Orian L.; Martins A.F.; Gomes A.E. *Phys. Rev. E* **2000**, *62*, 2228–2300; Martins, A.F.; Gomes, A.E.; Polimeno, A.; Orian, L. *Phys. Rev. E* **2000,** *62,* 2301–2309.
(14) Casquilho J.P.; Véron A.; Martins A.F. *Modelling Simul. Mater. Sci. Engng* **2006**, *14*, 1–14.
(15) Casquilho J.P. *Eur. Phys. J. E* **2005**, *17*, 413–422.
(16) Figueirinhas J.L.; Casquilho J.P. *Liq. Cryst.* **2005**, *32*, 727–734.
(17) Press W.H.; Teukolsky S.A.; Vetterling W.T.; Flannery B.P. *Numerical Recipes in Fortran*; Cambridge University Press: Cambridge, 1992.
(18) Grigutsch M.; Klopper N.; Scmiedel H.; Stannarius R. *Phys Rev E* **1994**, *49*, 5452–5461.
(19) Srajer G.; Fraden S.; Meyer R.B. *Phys. Rev. A* **1989**, *39*, 4828–4834.